AD-A163 184 FAILURE ANALYSIS OF A SODIUM HEAT PIPE WITH INTEGRAL LITHIUM FLUORIDE THE (U) ARIZONA STATE UNIV TEMPE DEPT OF MECHANICAL AND AEROSPACE ENG D L JACOBSON ET AL 1/1

UNCLASSIFIED SEP 85 AFWAL-TR-85-2063 F33655-81-C-2058 F/G 13/11 NL

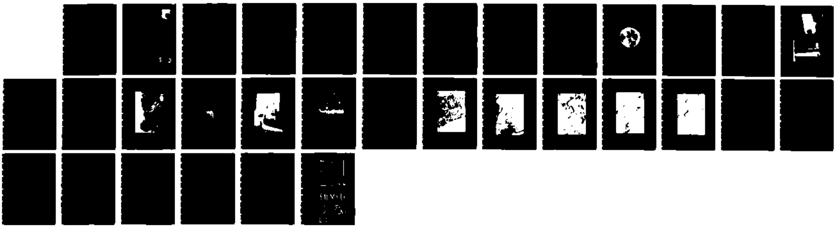

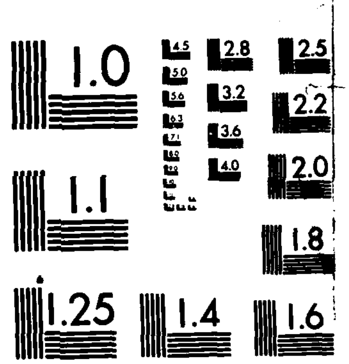

MICROCOPY RESOLUTION TEST CHART
NATIONAL BUREAU OF STANDARDS-1963-A

12

AFWAL-TR-85-2063

FAILURE ANALYSIS OF A SODIUM HEAT PIPE WITH INTEGRAL LITHIUM FLUORIDE THERMAL ENERGY STORAGE

D.L. Jacobson and P. Soundararajan

MECHANICAL AND AEROSPACE ENGINEERING
ARIZONA STATE UNIVERSITY
TEMPE, ARIZONA 85287

September 1985

FINAL REPORT FOR PERIOD JUNE 1984 - MARCH 1985

AERO PROPULSION LABORATORY
AIR FORCE WRIGHT AERONAUTICAL LABORATORIES
AIR FORCE SYSTEMS COMMAND
WRIGHT-PATTERSON AIR FORCE BASE, OHIO 45433

NOTICE

This technical report has been reviewed and is approved for publication.

VALERIE J. VAN GRIETHUYSEN
Power Technology Branch
Aerospace Power Division
Aero Propulsion Laboratory

HUGH C. BRIGGS, Major, USAF
Chief, Power Technology Branch
Aerospace Power Division
Aero Propulsion Laboratory

FOR THE COMMANDER

JAMES D. REAMS
Chief, Aerospace Power Division
Aero Propulsion Laboratory

Unclassified
SECURITY CLASSIFICATION OF THIS PAGE

AD-A163 184

REPORT DOCUMENTATION PAGE

1a. REPORT SECURITY CLASSIFICATION: UNCLASSIFIED	1b. RESTRICTIVE MARKINGS: None
2a. SECURITY CLASSIFICATION AUTHORITY	3. DISTRIBUTION/AVAILABILITY OF REPORT: Approved for Public Release; Distribution is Unlimited.
2b. DECLASSIFICATION/DOWNGRADING SCHEDULE	
4. PERFORMING ORGANIZATION REPORT NUMBER(S)	5. MONITORING ORGANIZATION REPORT NUMBER(S): AFWAL-TR-85-2063
6a. NAME OF PERFORMING ORGANIZATION: Arizona State University; 6b. OFFICE SYMBOL (If applicable)	7a. NAME OF MONITORING ORGANIZATION: Air Force Wright Aeronautical Laboratories Aero Propulsion Laboratory (AFWAL/POOS-3)
6c. ADDRESS (City, State and ZIP Code): Mechanical & Aerospace Engineering Dept. Materials Group, Tempe, AZ 85287	7b. ADDRESS (City, State and ZIP Code): Wright-Patterson AFB, Ohio 45433
8a. NAME OF FUNDING/SPONSORING ORGANIZATION: Aero Propulsion Laboratory; 8b. OFFICE SYMBOL (If applicable): AFWAL/POOS-3	9. PROCUREMENT INSTRUMENT IDENTIFICATION NUMBER: F33615-81-C-2058
8c. ADDRESS (City, State and ZIP Code): Wright-Patterson AFB, Ohio 45433	10. SOURCE OF FUNDING NOS.: PROGRAM ELEMENT NO. 62203F; PROJECT NO. 3145; TASK NO. 19; WORK UNIT NO. 49
11. TITLE (Include Security Classification): See reverse	

12. PERSONAL AUTHOR(S): Dean L. Jacobson, P. Soundararajan

13a. TYPE OF REPORT	13b. TIME COVERED	14. DATE OF REPORT (Yr., Mo., Day)	15. PAGE COUNT
Final	FROM Jun 84 TO Mar 85	September 1985	28

16. SUPPLEMENTARY NOTATION

17. COSATI CODES FIELD	GROUP	SUB. GR.	18. SUBJECT TERMS (Continue on reverse if necessary and identify by block number)
10	03		Heat Pipe, Sodium, Thermal Energy Storage
11	06		

19. ABSTRACT (Continue on reverse if necessary and identify by block number)

A sodium, 321 stainless steel heat pipe with three LiF filled Nb-1Zr tubes for thermal energy storage with 304 S.S. screen for wicking was thermal cycled to failure and then an analysis was performed to examine the failure. It was concluded that insufficient weld depth between an end cap and tube body permitted the propagation of a crack through a possible combination of thermal/corrosion failure, creep rupture and internal pressure. Crack propagation resulted in the abrupt rupture of the end cap. A number of possible scenarios for the process following a leak are discussed.

20. DISTRIBUTION/AVAILABILITY OF ABSTRACT: UNCLASSIFIED/UNLIMITED ☒ SAME AS RPT. ☐ DTIC USERS ☐	21. ABSTRACT SECURITY CLASSIFICATION: UNCLASSIFIED
22a. NAME OF RESPONSIBLE INDIVIDUAL: V. J. Van Griethuysen	22b. TELEPHONE NUMBER (Include Area Code): (513) 255-6235; 22c. OFFICE SYMBOL: AFWAL/POOS-3

DD FORM 1473, 83 APR — EDITION OF 1 JAN 73 IS OBSOLETE.

Unclassified
SECURITY CLASSIFICATION OF THIS PAGE

Block 11. Title:

FAILURE ANALYSIS OF A SODIUM HEAT PIPE WITH INTEGRAL LITHIUM FLUORIDE THERMAL ENERGY STORAGE

TABLE OF CONTENTS

LIST OF ILLUSTRATIONS

LIST OF TABLES

SECTION I

INTRODUCTION

1.1 Objectives

The Test Unit designated TT3 was a lithium-fluoride thermal energy storage (TES), sodium cylindrical heat pipe, built by General Electric Co. in 1972 and transferred to Xerox-EOS[1] and then to Arizona State University in June 1978.[1,2] ASU life-tested the TT3 from June 1978, to January 1983, when it failed with the rupture of an end cap from the heat pipe. The objective of this work was to identify the failure mode. The overall objectives of the TT3 test and subsequent failure analysis were to demonstrate the compatibility of LiF with Nb-1Zr, and Na with 304 (Screen), Nb-1Zr and 321 stainless steel, and to produce information which will lead to a better understanding of the failure mechanisms in liquid-metal heat pipes.[1]

1.2 Description of the TT3 Test Unit

The TT3 Test Unit was a tubular sodium heat pipe which contained three lithium-fluoride TES capsules. The heat pipe tube was 20 inches long and 2.25 inches in outside diameter, with a wicking structure securely attached to and lining the interior wall. This wick consisted of five layers of 100 mesh Type 304 stainless steel screen. The TES capsules, each sealed and containing 134 grams of LiF, had lengths of 10 inches and outside diameters of 0.81 inch. They were each wrapped with three layers of the 100 mesh screen and placed side by side in the midsection of the heat pipe. Several layers of screen were forced between the pipes producing firm contact. Figure 1 is a photograph of the open pipe prior to initial closure and operation. Containment of sodium inside the heat pipe was provided by two end caps electron-beam welded to the pipe. The heat pipe was 321 stainless steel and TES capsules were Nb-1Zr. Table 1 gives composition and properties. The sodium was approximately 99.5% pure. In an earlier text, the TES capsules were incorrectly described as being 304 S.S.[3]

A heat pipe system of this kind was to be eventually used in a satellite as an energy source and transfer mechanism for a Vuellemiur (VM) Cryo Cooler.[1,4] Solar thermal collectors would deliver heat to the TES heat pipe via a primary sodium heat pipe coupled to it. Through this "thermal train," the VM Cooler would receive a steady supply of energy during periods of occultation. The condition of alternating heating and cooling periods was simulated in the life tests (cyclic life tests). A Lindberg heavy duty tube furnace provided heat input to the TT3 and also maintained it at a uniform temperature during thermal charging.[1,2]

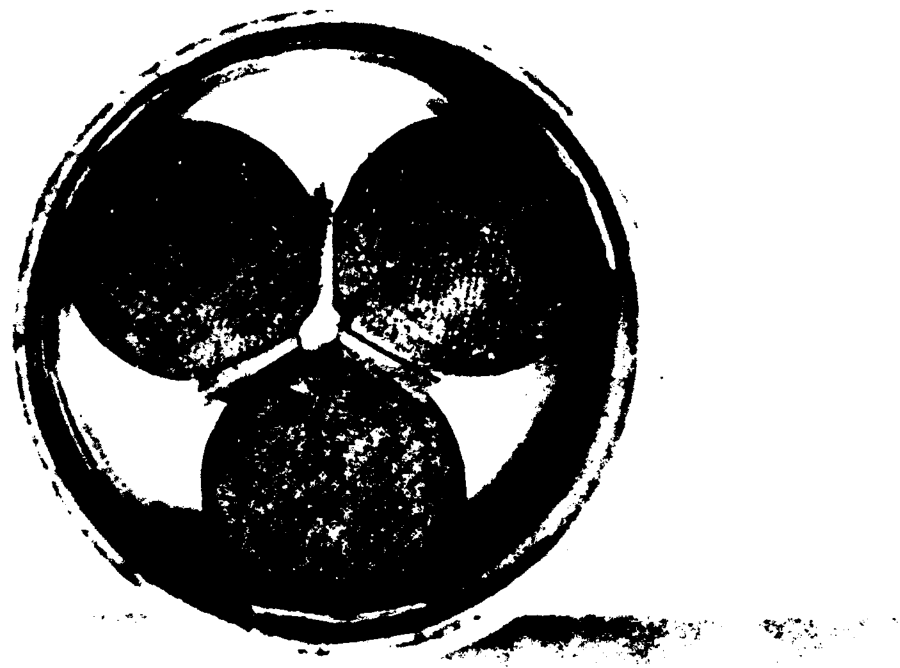

Figure 1. Interior of TT3 Test Unit Showing Three LiF Thermal Storage Cartridges. Heat Pipe OD Is 2.25 Inches.

Table 1

Composition and Properties of Type 321 Stainless Steel[5,6]

Elements	Nominal Composition (%)
Cr	17.0 - 19.0
Ni	9.0 - 12.0
Si	1.0 max.
C	0.08 max.
Mn	2.0 max.
Ti	5 X C min.
Fe	Balance

Properties	(70°F)	(1600°F)
Tensile Strength	85 kpsi	10625 psi
0.2% Yield Strength	30 kpsi	10125 psi
Elongation in 2 in.	55%	---
Reduction of Area	65%	---
Rockwell Hardness	B85	---

1.3 Operational History of the TT3 Test Unit

The TT3 was built by General Electric and life tested for 1 year. During that time it passed through 3150 cycles of thermal charging/discharging of the TES material and logged a total of 7875 hours of operation. After it was shut down, the unit was visually examined and radiographic pictures were taken of the three LiF capsules. No distortion of the capsules was observed, nor were there any indications of leaks. The TT3 appeared to be in good shape.[1,4]

The unit then was obtained by ASU in June 1978, where further life-testing was begun. During the 4 years of its operation at ASU, the TT3 passed through 560 cycles of thermal charging/discharging and logged a total of 4933 hours of operation. Therefore, over its lifetime, 3710 total cycles were completed and the cumulative test time was 12,808 hours.

During the life test at ASU the melting temperature of LiF was determined to be 1120°K (847°C) and the freezing temperature 1117°K. The Lindberg furnace kept the temperature of the heat pipe at approximately 15°K above the melting temperature of LiF during the heating portion of the cycle.

SECTION II

DESCRIPTION OF FAILURE AND PRELIMINARY EXAMINATIONS

2.1 Description of Failure

Failure of the TT3 Test Unit occurred during thermal charging when the unit was at a temperature of approximately 1120K. Visual examinations showed that the failure took place in the end cap-to-tube weld region. Failure occurred suddenly and took the form of an explosion.

2.2 Preliminary Examinations and Observations

The preliminary failure analysis consisted of visual examinations of the heat pipe tube and TES capsules, and identification of the important regions for later study. After the heat pipe had cooled, it was removed from the tube furnace. Then a number of pictures were taken of all the important parts and features. Two are shown in Figs. 2 and 3.

Three important observations were made at this time. The first was that a considerable amount of oxidation existed on several regions of the heat pipe outer wall. In two spots it looked as if pits were forming. The other two observations were: the TES capsules were intact (no deformation or leakage had occurred) and the heat pipe wick was not clogged or corroded.

With these observations made, the heat pipe tube was cut into six sections. Figure 4 shows this sectioning and describes the important features of each. Samples were then cut from each section and examined as described in the following sections. An optical microscope, a scanning electron microscope, with EDS and Auger electron Spectrometer were employed in the analysis.

2.3 Metallographic Examinations

The samples for optical microscopy (OM) were prepared in the following sequence: (1) mounted in Bakelite, (2) ground the exposed surfaces with a sequence of four abrasives (240 grit to 320, 400, then 600), (3) polished with a sequence of three lapping wheels (starting with 3 m diamond paste, to 1 micron diamond or alumina, and finished on 0.05 micron alumina) and finally (4) chemical-etched with glyceregia for approximately 4 minutes followed with Villela's Reagent for 30 seconds.

Samples prepared for the SEM were cleaned in trichloroethylene before the examination. Samples prepared for compositional analyses were not etched.

Figure 2. Failed End of the Heat Pipe with TES Capsule Exposed at the Tube End.

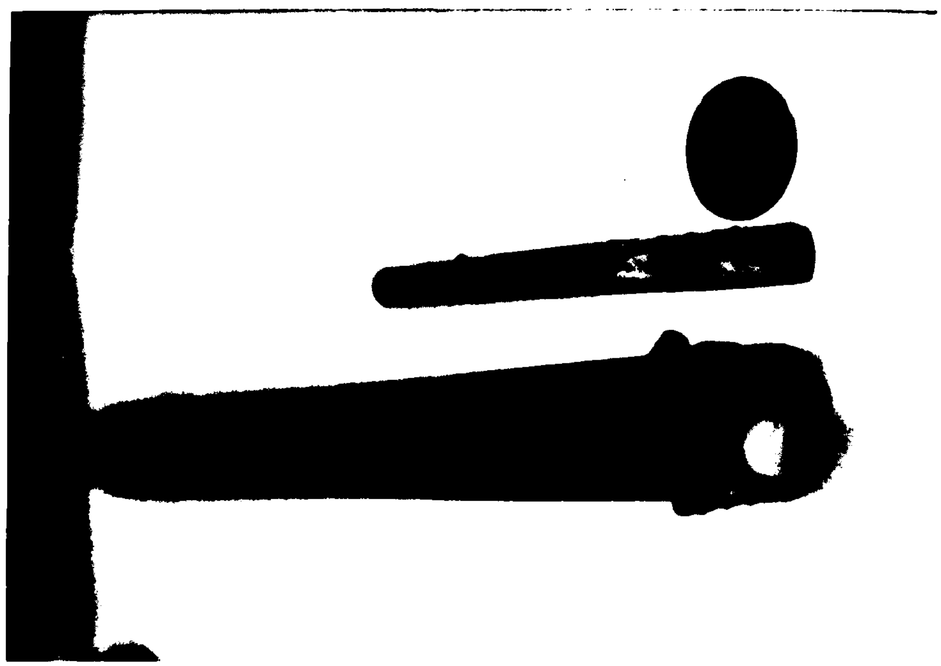

Figure 3. Top, Severed End Cap; Middle, Ejected TES Capsule; Bottom, Heat Pipe.

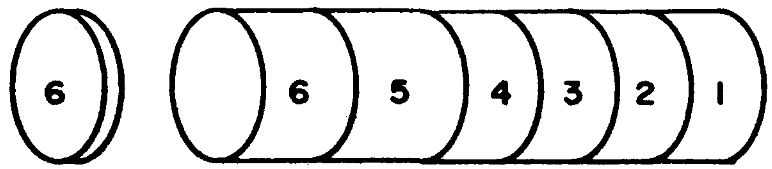

SECTION #6: FAILED END. TEN SAMPLES TAKEN FROM TUBE END AND CAP EDGES.

SECTIONS #5 & 4: PIT FORMATION ON EXTERIOR WALL ONE SAMPLE FROM EACH TAKEN.

SECTIONS #3 & 2: CLEAN BUT FOR OUTER SURFACE OXIDATION. NO SAMPLES TAKEN.

SECTION #1: UNFAILED END. TWELVE SAMPLES TAKEN FROM INTACT CAP-TO-TUBE WELD JOINT.

(OXIDATION EXISTED OVER MOST OF EXTERIOR SURFACE)

Figure 4. Heat Pipe Section Designations.

Section #6: Failed End. Ten Samples Taken From Tube End and Cap Edges.

Sections #5,8,4: Pit Formation on Exterior Wall One Sample From Each Taken.

Sections #3,8,2: Clean But For Outer Surface Oxidation. No Samples Taken.

Section #1: Unfailed End. Twelve Samples Taken From Intact Cap-To-Tube Weld Joint.

Examinations were begun on section 6, (Fig. 5) then proceeded to section 1, 4 and 5. Sections 2 and 3 were omitted because they showed no evidence of failure except for the outer surface scaling. Observations on sections 4 and 5 samples also did not show any sign of failure. The pit formation found on the outer tube surface was a small one as it did not travel far into the material. Examinations on section 6 samples showed a slight enlargement of the grains in the weld region.

The best and the most useful data were obtained through the examinations of section 1 samples. They show the geometry of the cap, tube and weld zone. Signs of the initial stages of weld cracking are observable which also most likely existed in the weld on the other end of the heat pipe which was severed at failure. Figure 6a is a sketch of section 1. Figure 6b shows micrographs of section 1 sample No. 1.3 at 200X. The sketch in Fig. 6a serves to highlight five important features: crack length and orientation, gap width, diameter and curvature at the base of the crack, grain discoloration and pitting along grain boundaries, grain size and tensile stressing.

The crack which begins at point A, travels into 49% of the weld depth, A to D, for sample 1.3. It was the longest found. Shorter cracks are also apparent in the section 1 samples along the gap region from B to A with the smallest at point B and growing progressively larger toward A. These cracks tend to run along the grain boundaries. The sketch in Fig. 6a depicts this feature. The gap between tube and cap, from point B to A has been observed in all but one of the samples. It is the unwelded section of contact. This space may have been the result of continuous loading on the cap, but more likely existed at the time of welding. In any case, it allowed liquid sodium, or sodium vapor to easily come into contact with the weld. Also, some widening of the gap at point A (crack base) is apparent. This may be an indication of corrosion. Corrosion is also indicated by the pitting and discoloration (relative darkening) of the grains along the regions C-B and B-A. The weld region extends from A to D (Fig. 6a) and this was made by electron beam.[2] This type of

Figure 5. Micrograph of a Section 6 Sample at 200X; Left Side is the Weld; Right Side is the Tube End.

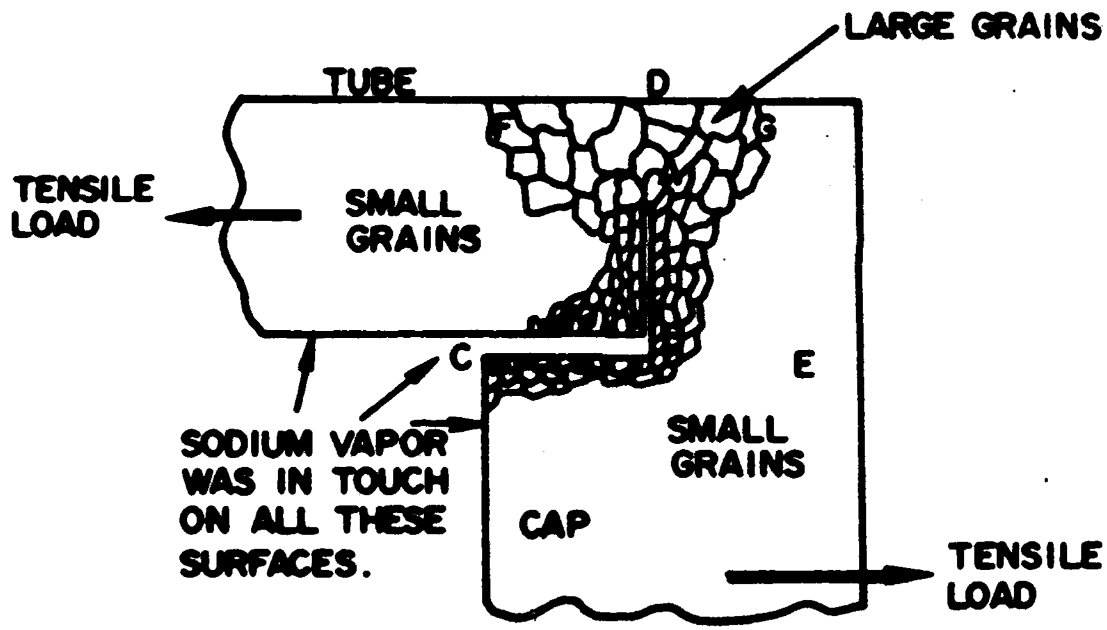

REPRESENTATIVE SKETCH OF SECTION 1 SAMPLE

Figure 6a. Representative Sketch of Section 1 Sample.

Figure 6b. Micrograph Composite of Sample 1.3 End Cap to Tube Weld Zone (200X).

Figure 6c. Micrograph of Tube/Cap Joint Showing Cracking Behavior (200X).

welding may account for the size of the grains being larger in the weld region than in the adjacent material (this variation is seen more clearly in section 6 micrographs, for example Fig. 5). The average weld length calculated from the section 1 samples is 0.315 mm. The data from all the section 1 samples are given in Table 2.

Table 2

Data from All Section 1 Samples

Sample No.	l_c	t_w	w_g
1.1	24	59	1.5
1.2	0	32	1.0
1.3	31	63	1.0
1.4	16	58	3.0
1.5	-	-	-
	used for AES and EDS		
1.6	-	-	-
1.7	19	61	2.0
1.8	0	50	1.0
1.9	30	69	1.0
1.10	18	62	4.0

- All data in mm from 200X micrographs.
- l_c = crack length
  t_w = total weld thickness (AD)
  w_g = gap width at point A (crackbase)
- outside radius of heat pipe r_o = 1.125 inches

2.4 Observations Obtained with the Scanning Emission Microscope

The Scanning Emission Microscope (SEM) samples were from section 6 of the heat pipe. SEM pictures of a cap sample and a tube sample are given in Fig. 7. The micrographs obtained are of the fracture surfaces. Two important features of these surfaces are: (1) Macroscopically, there appears to be little plastic deformation. The SEM pictures exhibit dimples on the fracture surfaces which indicate that the material is ductile and the fracture was ductile. (2) There were some white areas in the SEM pictures which could be oxides.

2.5 Chemical Analyses

Chemical analyses were performed with the SEM Energy Dispersive Spectrometry (EDS) and Auger Electron Spectroscopy

Figure 7a. Weld and Non-Weld Regions Along Cap Edge (102X).

Figure 7b. Cap Edge Weld Region (1030X).

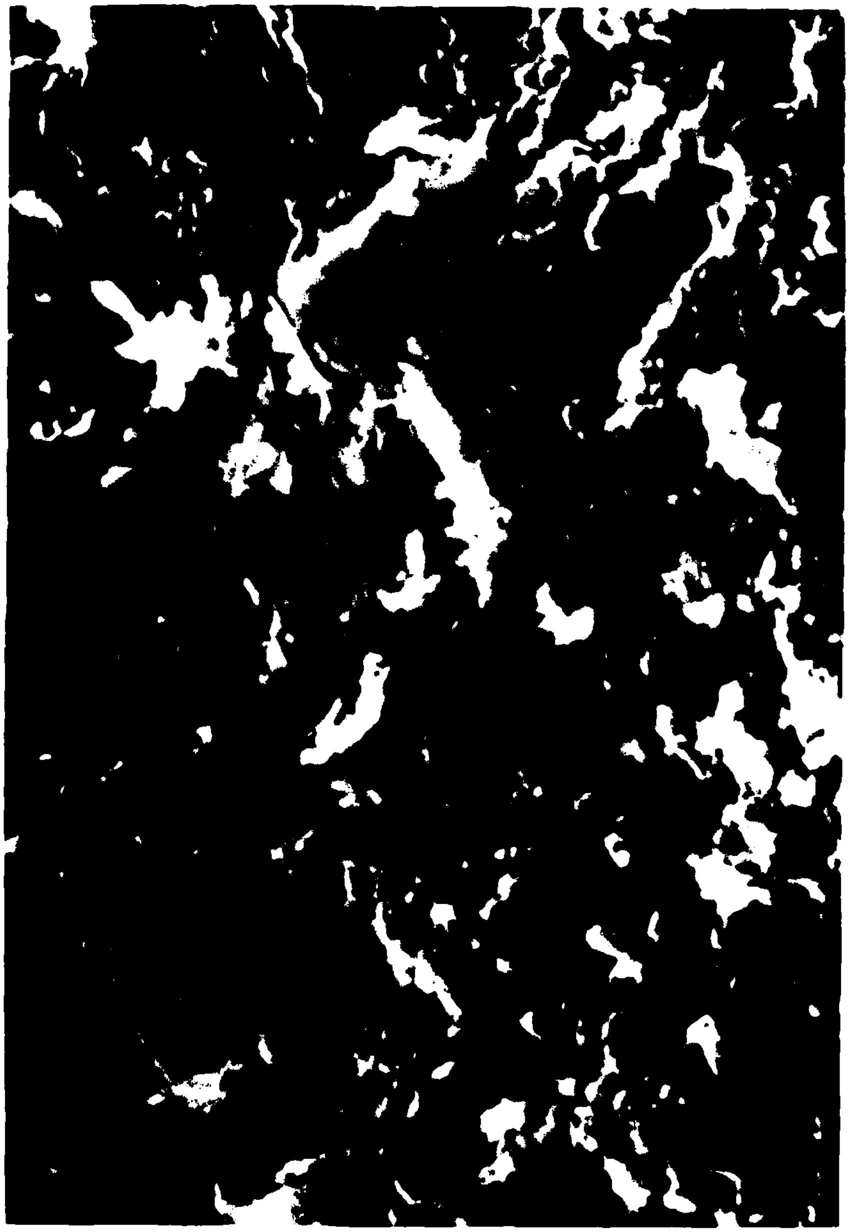

Figure 7c. Non-Welded Region of Cap Edge (1040).

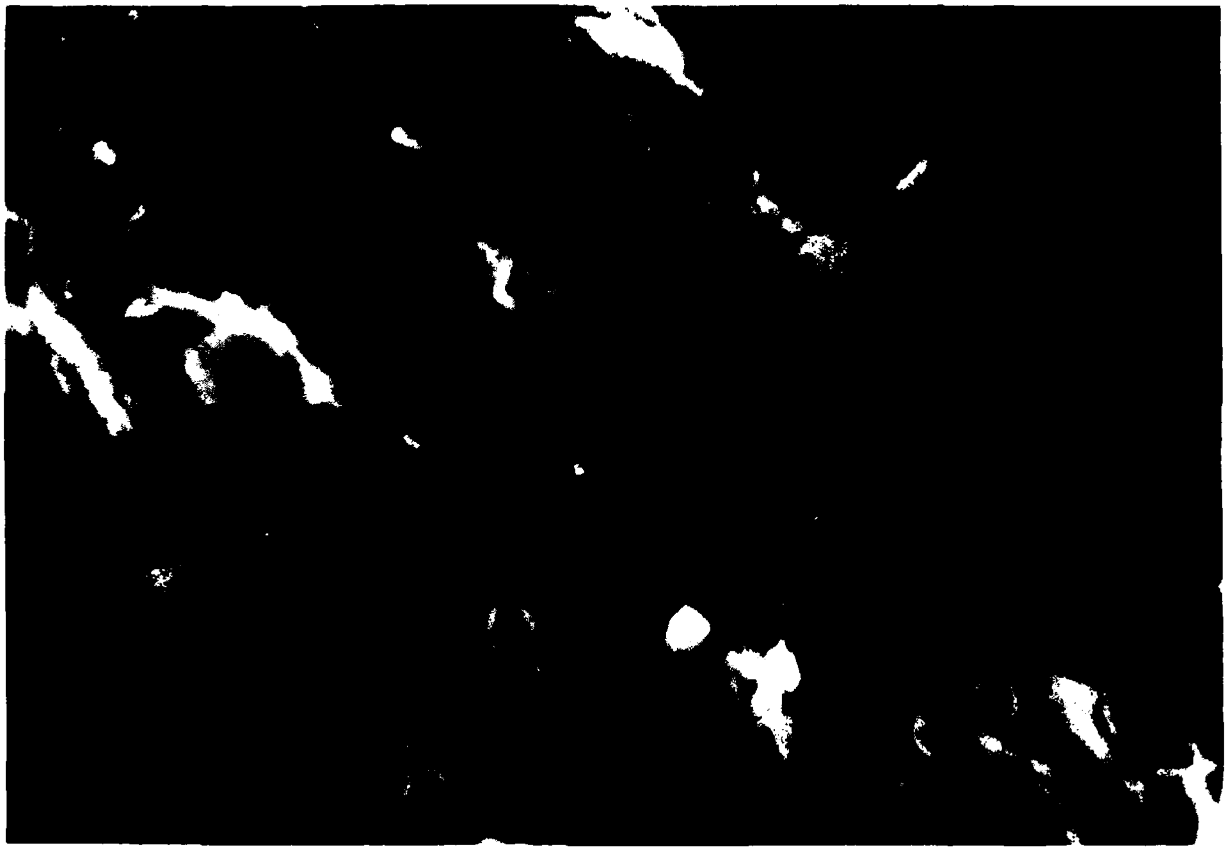

Figure 7d. Tube Edge Weld Region (2900X).

Figure 7e. Tube Edge Unwelded Region (1200X).

(AES). The objectives were to verify the heat pipe material as Type 321 stainless steel and to look for impurities in the material such as foreign elements possibly introduced during welding, or corrosion products containing oxygen or carbon. The EDS analysis was performed by the Materials Laboratory at the Wright-Patterson Air Force Base in Dayton, Ohio[7] and by ASU. AES was performed at ASU.

The combined results of both analyses are shown in Table 3. The areas examined were the weld regions near the crack. In both analyses the heat pipe material was quantitatively shown to be Type 321 stainless steel. There is a slight difference between the compositions determined through each technique, but this can be attributed to a difference in either detection levels or the precise areas examined by each. Samples from section 1, No's. 1.5 and 1.6, were used for these analyses.

There was no trace of sodium with either technique. This indicates that liquid sodium did not react chemically to form compounds with any elements of stainless steel. Carbon was found in the samples examined, but only less than the maximum specified for Type 321 stainless steel. Neither method could detect oxygen, which is very important even in very small amounts (5 ppm) in producing a corrosive sodium situation.[3,8]

Table 3

Material Verification by AES and EDS on Section 1 Samples

	Weight %		
Compositional Element	AES on Sample 1.5	EDS on Sample 1.6	321 Nominal
Si	0.71	0.77	1.0 max
Ti	0.64	0.80	5 X C min
C	22.79	18.13	17.0-19.0
Ni	8.74	10.93	9.0-12.0
Fe	67.10	69.36	Balance

* Examination areas were weld regions near the crack.

at the condenser end, allowing a pressure buildup equal to the sum of the partial pressures.[12] At 700°C the pressure should not be sufficient for rupture even though the weld zone was found to be very thin as discussed earlier.

Another possibility for catastrophic failure is an air leak into the pipe in the region of the hydrogen gas accumulation. This was suggested by Mr. Jim Morris.[13] The ends of the heat pipe were probably slightly cooler than the center owing to the nature of the tube furnace and the thermal insulation. The hydrogen would accumulate in the vicinity of the end caps and therefore the weld regions. With the occurrence of a crack, the air, being at a pressure greater than that of the sodium vapor plus hydrogen, could rush in with an ensuing hydrogen-oxygen explosion. The hydrogen can accumulate during operation in the portion of the heat pipe from which the hydrogen is being swept since the partial pressure of hydrogen will essentially be zero in that region. As this occurs, the condenser will continue to shrink.

It is felt that the failure could have been avoided with any number of improved weld designs. The weld thickness was found to be as little as 0.01 in. and could have been thinner elsewhere. In general the 321 S.S., sodium system appeared to perform satisfactorily as evidenced by the absence of corrosion, in general, in the heat pipe. It is important though to provide for high purity sodium and to fabricate the heat pipes with exceptionally clean internal surfaces in order to maintain the sodium purity and obtain maximum life time. The thermal energy storage capsules showed no evidence of corrosive attack on the sodium side. The salt-container corrosion analysis will be reported on later.

ACKNOWLEDGEMENTS

The authors would like to thank Dr. E.T. Mahefkey and Valerie J. van Griethuysen of AFWAL for their support of this work and Mr. Keith A. Quaranta who assisted in much of the experimental work as part of a Senior Project.

SECTION IV

CONCLUSION

A tensile stress existed in the cap-to-tube weld region but the maximum tensile stress (σ_{max} = 2300 psi) was much lower than the yield strength and the failure was apparently time dependent. The chemical species in the environment responsible for corrosion were not definitely present in large quantities (from AES and EDS results). The heat pipe material suffered no general corrosion. The fracture was microscopically brittle in nature (as seen from the OM and SEM pictures). The cracks generally followed grain boundaries and were discolored but the crack tips were not preceded by any apparent corrosion nor were there detectable corrosion products in the grain boundaries.

Whatever the crack mechanism was, once the heat pipe wall was penetrated, air (oxygen and water vapor) rapidly entered the heat pipe with an ensuing catastrophic severing of the heat pipe end cap. The fracture surface appeared to have undergone an impact-like rupture and the scanning emission micrographs showed that the material was ductile. Some oxide formation is apparent on the fracture surface and probably occurred while the surface was still hot following rupture.

The analyses performed were not absolutely conclusive in regard to the failure mechanism. It appears that a combination of thermal stresses and oxygen contaminated sodium led to thermal/corrosion fatigue or creep fracture. The actual internal heat pipe pressure is unknown, and therefore such contributing stresses are unknown.

Don Ernst[12] suggested that a small crack in the weld area could have allowed air to enter the pipe with an ensuing pressure rise and rupture. This would require the crack to plug up allowing a three or four atmosphere pressure rise at temperature. It may have been possible for a crack to open at low temperature and close at high temperature as a result of thermal stress variations in the region of the end cap weldment.

It should be noted that the internal surfaces did not exhibit oxide formation and that performance degradation was not detected. No sodium leaks were found during periodic examination of the heat pipe.

It is also known that because of the permeability of stainless steel to hydrogen that at room temperature sodium hydride probably exists in the heat pipe. Experience at RCA suggested that upon heating, the hydrogen (which is a non-condensible gas) and the sodium vapor segregate with the hydrogen

the maximum stress in the weld region is about 23% of the yield stress and a purely mechanical failure by stress overload was not considered likely.

From the data in Table 2, the crack length versus gap width/diameter of curvature at A can be plotted and is inversely proportional to the gap width. This relationship is similar to a characteristic trend in brittle fracture cracks.

Liquid-Metal Embrittlement (LME) is not a time dependent failure mode[9] and if LME were responsible failure would probably have occurred much earlier in the life testing.

Hydrogen Embrittlement (HE) is not likely since austenitic steels highly resist HE because the fact-centered structure is relatively impermeable to atomic hydrogen[9]. The only source of hydrogen in the pipe would be by diffusion from the atmosphere through the pipe walls. Also, niobium is a good hydrogen-getter especially at high temperatures.

The OM micrographs of the samples showed evidence of small amounts of corrosion as pits and discoloration (see Figure 6). The AES and EDS analyses did not show any chemical species responsible for this corrosion. For stress-corrosion, even a few ppms of the corrosive species are sufficient.[9] In this case a few ppm of oxygen in the sodium may have provided sufficient corrodant. AES and EDS techniques were not able to detect such small levels. SEM pictures of the fracture surface give a clue that the corrosion agent could have been oxygen. The presence of oxygen in the sodium of TT3 unit is suspected as (1) the sodium was only 99.5% pure and (2) there is a possibility that additional oxygen entered the heat pipe during fabrication and charging of the unit. It has been found that as little as 5 ppm of oxygen in sodium can transform a system from a passive one to an actively corrosive system.

Thermal/Corrosion Fatigue requires a small fluctuating stress, and at 1100K and the inherent crack geometry makes the required stress difficult to determine. The transient thermal gradients imposed during thermal cycling provided a low stress amplitude providing time for environmental interaction with the sodium and/or sodium oxide. Evidence of fatigue through a rubbed region was not found but the possibility for fatigue still exists since such a region could be exceedingly small.

Creep fracture also involves plastic strain below the yield strength. Its occurrence should have resulted in a thinning of the weld region and possibly a dimpled fracture surface in a localized region. These characteristics were not found but the possibility of creep fracture should not be ruled out.

SECTION III

EVALUATION OF POSSIBLE CAUSES AND FORMULATION OF FAILURE MODE

Formulation of the failure mode was based primarily on 1) observations and data obtained through the metallographic and chemical examinations, 2) the known composition and high-temperature properties of Type 321 stainless steel and 3) the consideration of a number of possible causes of the failure, which are discussed in the following section.

3.1 Possible Modes of Failure

During the failure analysis, a number of forms of failure were considered; (1) general corrosion, (2) intergranular corrosion, (3) mechanical stress overload, (4) creep rupture, (5) thermal/corrosion fatigue, (6) liquid-metal embrittlement, (7) hydrogen embrittlement, (8) stress-corrosion cracking.

General corrosion of the weld surface at point A in Figure 6a was considered but ruled out following the detailed examination of all section 1 samples. These examinations, previously discussed, showed that the thickness of the unfractured weld region was not the same in all samples; it would have been had general corrosion occurred.[9,10] The general internal surfaces and wick appeared metallographically to have undergone no corrosive attack. Thus, a failure based solely on general corrosion is not likely.

Intergranular corrosion occurs due to improper heat treatment of stainless steels. For austenitic alloys, the sensitizing temperature range is 700 to 1250K. In this case no carbides or other precipitates were found along the grain boundaries. Weld decay by intergranular corrosion was not found because there was no significant corrosive attack in zones slightly away from the weld, so intergranular corrosion failure was ruled out. In the cracks, the discoloration, indicating corrosion did not precede the cracks.

During the operation of TT3, a tensile stress existed in the weld, due to the sodium vapor pressure inside the heat pipe and possible non-condensible gasses evolved. As sample 1.3 has the largest crack length (Table 2), it would have experienced the maximum stresses in the weld region. For this sample, the minimum nominal stress across the weld region A-D (Fig. 6a) for the maximum temperature of 1200K which corresponds to a sodium vapor pressure P of 12.64 psi, has been calculated to be approximately 577 psi. A very conservative estimate of the stress concentration factor is about 4.0 for the point A.[11] Therefore, the maximum stress σ_{max}, which occurs at A, is 2308 psi. The yield stress σ_{yp} at 1200K for Type 321 stainless steel is 10125 psi. Hence

REFERENCES

1. Richter, R., Solar Collector Thermal Power System (SCTPS) First Interim Report, EOS Report 4074-I-1, January 14, 1972, Appendix E.

2. Richter, R., Solar Collector Thermal Power System (SCTPS) AFAPL-TR-74-89, Vol. III, Sect. IV, pp. 89-160.

3. Jacobson, D. and Soundararajan, S., "Failure Analysis of a Sodium Heat Pipe with Integral Lithium Fluoride Thermal Energy Storage," Proceedings of 5 IHPC, Part I, pp. 175-180.

4. Jacobson, Dean L., "Lithium-Fluoride, Sodium Heat Pipe Thermal Train Subsystem Life Test," FY 1980 Report on Analytical and Experimental Investigations of Heat Transfer, Materials, and Thermodynamic Problems, Arizona State University, August 20, 1980; prepared for AFWAL, AFAPL, WPAFB, Ohio.

5. Mark's, Mechanical Engineer's Handbook, 8th Ed.

6. Department of Defense, Aerospace Structural Metals Handbook, Mechanical Properties Data Center, Belfour Stulen, Inc., 1982.

7. Saul, G., AFWAL/MLS 83-40, May 1983.

8. Foust, O.J., (Editor), "Sodium Purification, Material, Heaters, Coolers, and Radiators," Sodium-NaK Engineering Handbook, Vol. 5, Gordon and Breach, Science Publishers, Inc., 1979.

9. American Society for Metals, "Failure Analysis and Prevention," Metals Handbook, 5th Ed., Vol. 10, 1975.

10. Nevzorov, B.A., Corrosion of Structural Materials in Sodium, Weiner Bindery Ltd., Jerusalem, 1970.

11. Spotts, M.F., Design of Machine Elements, 5th Ed., Prentice-Hall, Inc., Englewood Cliffs, New Jersey, 1978.

12. Ernst, D., Thermocore; Private Communications.

13. Morris, J., Arizona State University, Private Communications.

U.S.Government Printing Office: 1986 — 646-067/40634

END

FILMED

2-86

DTIC